The Canadian Mineralogist
Vol. 54, pp. 625-634 (2016)
DOI: 10.3749/canmin.1500058

RAYGRANTITE, $Pb_{10}Zn(SO_4)_6(SiO_4)_2(OH)_2$, A NEW MINERAL ISOSTRUCTURAL WITH IRANITE, FROM THE BIG HORN MOUNTAINS, MARICOPA COUNTY, ARIZONA, USA

HEXIONG YANG§, MARCELO B. ANDRADE, ROBERT T. DOWNS, RONALD B. GIBBS, AND ROBERT A. JENKINS

Department of Geosciences, University of Arizona, 1040 E. 4th Street, Tucson, Arizona 85721, U.S.A.

ABSTRACT

A new mineral species, raygrantite, ideally $Pb_{10}Zn(SO_4)_6(SiO_4)_2(OH)_2$, has been found in the Big Horn Mountains, Maricopa County, Arizona, USA. Associated minerals are galena, anglesite, cerussite, lanarkite, leadhillite, mattheddleite, alamosite, hydrocerussite, caledonite, and diaboleite. Raygrantite crystals are bladed with striations parallel to the elongated direction (the **c** axis). Twinning (fish-tail type) is pervasive on (1 2 $\bar{1}$). The mineral is colorless, transparent with white streak, and has a vitreous luster. It is brittle and has a Mohs hardness of ~3; cleavage is good on {120} and no parting was observed. The calculated density is 6.374 g/cm^3. Optically, raygrantite is biaxial (+), with $n_\alpha = 1.915(7)$, $n_\beta = 1.981(7)$, $n_\gamma = 2.068(9)$, $2V_{meas} = 76(2)°$, and $2V_{calc} = 85°$. It is insoluble in water, acetone, or hydrochloric acid. An electron microprobe analysis yielded the empirical formula $Pb^{2+}_{9.81}Zn^{2+}_{0.93}(S_{1.00}O_4)_6(Si_{1.05}O_4)_2(OH)_2$.

Raygrantite is a new member of the iranite mineral group. It is triclinic, with space group $P\bar{1}$ and unit-cell parameters a 9.3175(4), b 11.1973(5), c 10.8318(5) Å, α 120.374(2), β 90.511(2), γ 56.471(2)°, and V 753.13(6) Å^3. Its crystal structure, refined to $R_1 = 0.031$, is characterized by slabs that lie parallel to (120) of SO_4 and SiO_4 tetrahedra with $ZnO_4(OH)_2$ octahedra, held together by Pb^{2+} cations displaying a wide range of Pb–O bond distances. The discovery of raygrantite indicates that, in addition to complete OH–F and Cu–Zn substitutions, there is also a complete substitution between $(CrO_4)^{2-}$ and $(SO_4)^{2-}$ in the iranite group of minerals, pointing to the possible existence of a number of other $(SO_4)^{2-}$-bearing iranite-type phases yet to be found or synthesized.

Keywords: raygrantite, iranite, hemihedrite, crystal structure, X-ray diffraction, Raman spectra.

INTRODUCTION

A new mineral species, raygrantite, ideally $Pb_{10}Zn(SO_4)_6(SiO_4)_2(OH)_2$, has been found in Arizona, USA. The mineral is named in honor of Dr. Raymond W. Grant, a retired professor of geology at Mesa Community College in Mesa, Arizona. Dr. Grant's primary scientific interest is minerals found in Arizona. His publications include several articles on Arizona mineral localities, the Checklist of Arizona Minerals, and the 3rd edition of Mineralogy of Arizona. Ray Grant is the past and current President of the Mineralogical Society of Arizona, past Chairman of the Flagg Mineral Foundation, and a principal organizer of the Arizona Mineral Symposium. The new mineral and its name have been approved by the Commission on New Minerals and Nomenclature and Classification (CNMNC) of the International Mineralogical Association (IMA2013-001). Part of the co-type samples has been deposited in the University of Arizona Mineral Museum (Catalogue # 19345) and the RRUFF Project (deposition # R120151, www://rruff.info/raygrantite). This paper describes the physical and chemical properties of raygrantite and its structural characterization based on single-crystal X-ray diffraction and Raman spectroscopic data.

SAMPLE DESCRIPTION AND EXPERIMENTAL METHODS

Occurrence, physical and chemical properties, and Raman spectra

Raygrantite was found at the Evening Star mine (a former underground Cu-V-Pb-Au-Ag-W mine, also previously called Old Queen Group or Silver Queen mine), Big Horn District, Big Horn Mountains, Maricopa County, Arizona, USA (Lat. 33°70′ N,

§ *Corresponding author e-mail address*: hyang@u.arizona.edu

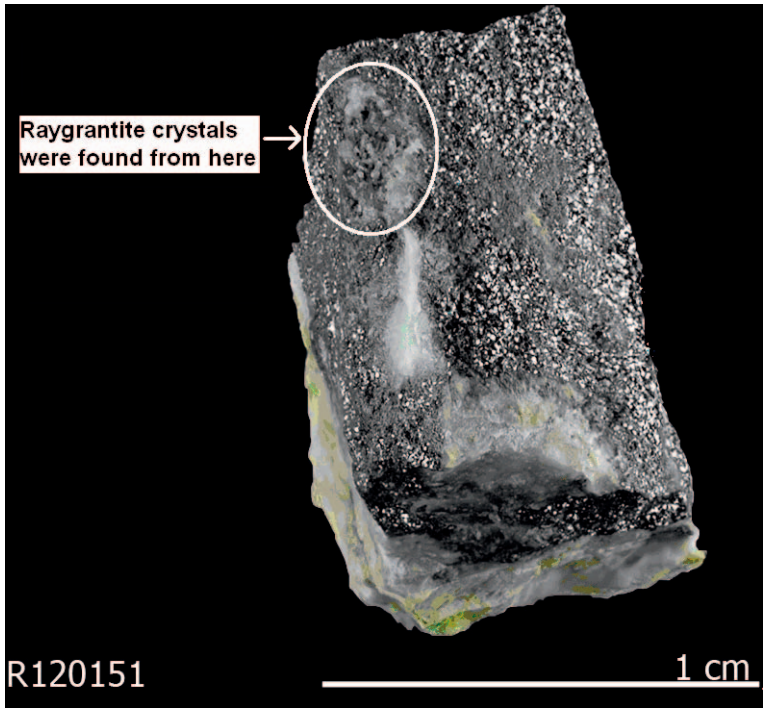

FIG. 1. The rock sample on which the raygrantite crystals were found.

Long. 113°21′W). The crystals were found within a small cavity in a mass of galena (Fig. 1). Associated minerals include galena, anglesite, cerussite, lanarkite, leadhillite, mattheddleite, alamosite, hydrocerussite, caledonite, and diaboleite. Also, among the "rind" are fornacite, iranite, phoenicochroite, cerussite, and murdochite. Raygrantite is believed to have a secondary origin as a remnant of a galena-pyrite-chalcopyrite vein. Mineral occurrences in the Big Horn district are gold-rich, basement-hosted narrow quartz pods and veins associated with late Cretaceous intrusives (Allen 1985).

Raygrantite crystals are bladed and elongated along the **c** axis (up to 0.05 × 0.10 × 0.30 mm), with striations parallel to the **c** axis (Fig. 2). Twinning (fish-tail type) is pervasive on (1 2 $\bar{1}$), with the twin axis along [0 1 0] (Fig. 3). The mineral is colorless in transmitted light, transparent with white streak, and has a vitreous luster. It is brittle and has a Mohs hardness of ~3; cleavage is good on {120} and no parting was observed. Fractures are uneven. The calculated density is 6.37 g/cm^3. Optically, raygrantite is biaxial (+), with $n_\alpha = 1.915(7)$, $n_\beta = 1.981(7)$, $n_\gamma = 2.068(9)$, $2V_{meas} = 76(2)°$, and $2V_{calc} = 85°$. Dispersion is strong ($r > v$) and absorption is $Z > Y > X$. The Gladstone Dale compatibility index is 0.04 (good). Raygrantite is insoluble in water, acetone, or hydrochloric acid.

The chemical composition of raygrantite was determined with a CAMECA SX100 electron microprobe operating at 20 kV and 20 nA with the beam diameter of ~1 μm. The standards include wollastonite for Si, barite for S, wulfenite for Pb, and ZnO for Zn, yielding an average composition (wt.%) (18 points) of SiO_2 4.30(19), SO_3 16.49(33), PbO 74.91(34), ZnO 2.59(11), H_2O 0.62 (added to bring the total close to the ideal value), and total = 98.81(45). The presence of OH in raygrantite was also confirmed by Raman spectroscopic measurements and structure determination (see below). Trace amounts of Cu, Cr, and F were observed from WDS, but they are under the detection limits of electron microprobe analysis. The resultant chemical formula, calculated on the basis of 34 O atoms (from the structure determination), is $Pb_{9.81}Zn_{0.93}(S_{1.00}O_4)_6(Si_{1.05}O_4)_2(OH)_2$, which can be simplified as $Pb_{10}Zn(SO_4)_6(SiO_4)_2(OH)_2$.

The Raman spectrum of raygrantite was collected from a randomly oriented crystal with a Thermo Almega microRaman system, using a 532-nm solid-state laser with a thermoelectric cooled CCD detector. The laser is partially polarized with a 4 cm^{-1} resolution and a spot size of 1 μm.

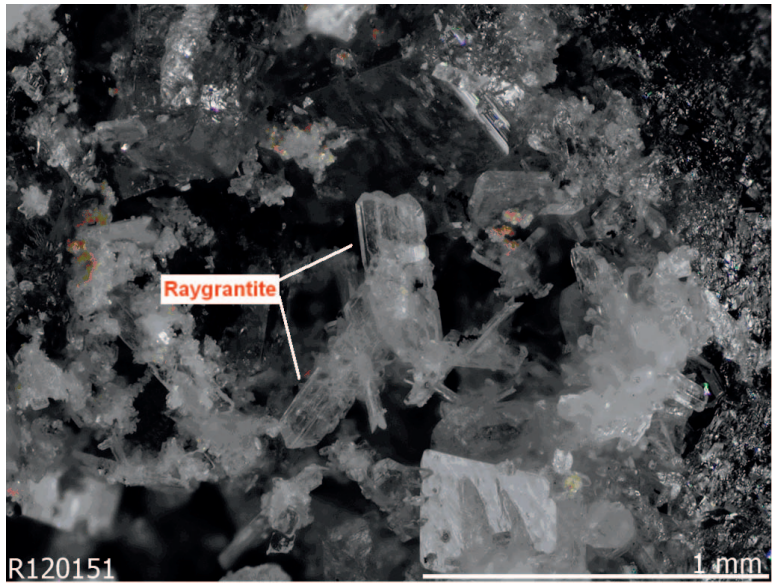

FIG. 2. A microscopic view of raygrantite crystals in a vug.

X-ray crystallography

Both the powder and single-crystal X-ray diffraction data for raygrantite were collected using a Bruker X8 APEX2 CCD X-ray diffractometer equipped with graphite-monochromatized Mo$K\alpha$ radiation. However, due to severe overlaps, it is difficult to unambiguously index all the powder X-ray diffraction peaks. Thus, no unit-cell parameters were determined from the powder X-ray diffraction data. Listed in Table 1 are the measured powder X-ray diffraction data, along with those calculated from the determined structure using the program XPOW (Downs *et al*. 1993).

FIG. 3. A backscattered electron image of fish-tail type twinning in raygrantite.

TABLE 1. POWDER DIFFRACTION DATA FOR RAYGRANTITE

Experimental		Theoretical		
Intensity	*d*-spacing (Å)	Intensity	*d*-spacing (Å)	*h k l*
9	5.521	9.40	5.4655	1 1 1
56	4.753	60.42	4.7761	1 2 0
26	4.608	28.59	4.6153	$\bar{1}$ $\bar{2}$ 2
32	4.288	28.48	4.2852	2 2 0
17	3.872	24.97	3.8800	2 0 1
18	3.604 (2 overlaps)	11.15	3.6297	$\bar{1}$ $\bar{3}$ 2
		18.91	3.5987	2 0 0
27	3.492 (3 overlaps)	11.11	3.4987	2 $\bar{2}$ 2
		13.17	3.4878	0 $\bar{1}$ 3
		16.76	3.4857	2 0 2
25	3.362	22.82	3.3614	$\bar{1}$ $\bar{2}$ 3
63	3.267	100.00	3.2743	1 $\bar{2}$ 2
100	3.102 (3 overlaps)	76.06	3.1139	1 0 3
		60.92	3.1055	3 2 0
		15.81	3.0876	$\bar{1}$ 1 1
29	2.996 (3 overlaps)	12.99	3.0055	1 $\bar{2}$ 3
		7.97	2.9841	$\bar{2}$ $\bar{1}$ 2
		9.88	2.9529	$\bar{2}$ 0 1
35	2.851	46.00	2.8590	0 2 1
31	2.783	45.34	2.7926	$\bar{2}$ $\bar{4}$ 2
31	2.707	33.59	2.7185	$\bar{2}$ $\bar{2}$ 3
20	2.648	17.20	2.6544	2 3 1
16	2.557 (2 overlaps)	6.40	2.5659	0 $\bar{3}$ 4
		5.04	2.5425	3 0 2
15	2.535 (3 overlaps)	10.52	2.5396	$\bar{3}$ $\bar{2}$ 2
		7.03	2.5078	3 2 2
		5.54	2.4875	0 3 0
7	2.379 (2 overlaps)	7.28	2.3991	3 0 0
		3.71	2.3869	$\bar{1}$ 0 3
10	2.312 (3 overlaps)	8.23	2.3238	3 0 3
		6.49	2.3142	4 3 0
		6.93	2.3065	3 1 3
19	2.270	19.75	2.2826	0 $\bar{4}$ 2
15	2.155 (3 overlaps)	9.99	2.1649	0 0 4
		10.68	2.1635	2 2 3
		5.85	2.1565	3 3 2
21	2.128 (3 overlaps)	13.17	2.1371	$\bar{4}$ $\bar{4}$ 2
		7.77	2.1354	0 $\bar{2}$ 5
		8.59	2.1163	$\bar{3}$ 0 1
10	2.062	17.43	2.0676	$\bar{1}$ $\bar{4}$ 5

Single-crystal X-ray diffraction data were collected from a nearly equidimensional twinned crystal ($0.05 \times 0.04 \times 0.04$ mm) with frame widths of 0.5° in ω and 30 s counting time per frame. Figure 4 is the reciprocal plot of X-ray reflections viewed down **c***. The two twin components are related to each other by the twin law ($\bar{1}$ 1 0, 0 1 0, 0 $\bar{1}$ $\bar{1}$). All reflections were indexed on the basis of a triclinic unit-cell (Table 2) and processed with the software TWINABS (Sheldrick 2007). The intensity data were corrected for X-ray absorption using the Bruker program SADABS. The systematic absences of reflections suggest possible space group *P*1 or $P\bar{1}$. The crystal structure was solved and refined using SHELX97 (Sheldrick 2008) based on space group $P\bar{1}$, because it produced the better refinement statistics in terms of bond lengths and angles, atomic displacement parameters, and *R* factors. The positions of all atoms were refined with anisotropic displacement parameters. The H atoms were not located from the difference Fourier maps.

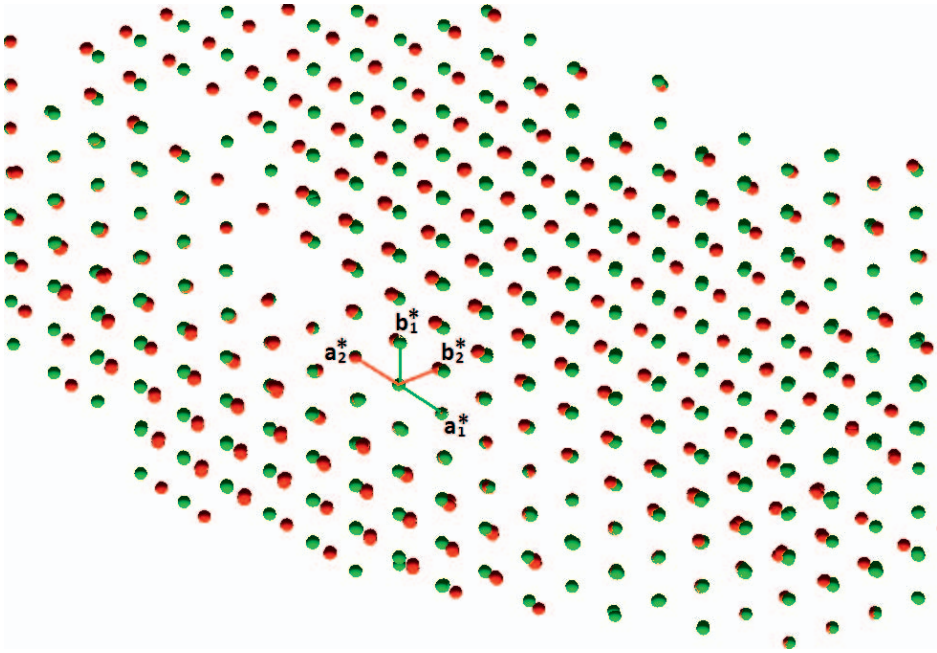

FIG. 4. A reciprocal plot of X-ray reflections of raygrantite viewed down **c***, showing the two twin components.

TABLE 2. COMPARISON OF CRYSTALLOGRAPHIC DATA FOR RAYGRANTITE, IRANITE, AND HEMIHEDRITE

	raygrantite	iranite	hemihedrite
Ideal chemical formula	$Pb_{10}Zn(SO_4)_6(SiO_4)_2(OH)_2$	$Pb_{10}Cu(CrO_4)_6(SiO_4)_2(OH)_2$	$Pb_{10}Zn(CrO_4)_6(SiO_4)_2F_2$
Crystal symmetry	Triclinic	Triclinic	Triclinic
Space group	$P\bar{1}$ (#2)	$P\bar{1}$ (#2)	$P\bar{1}$ (#2)
a(Å)	9.3175(4)	9.5416(4)	9.497(3)
b(Å)	11.1973(5)	11.3992(5)	11.443(5)
c(Å)	10.8318(5)	10.7465(4)	10.841(4)
α(°)	120.374(2)	120.472(2)	120.50(4)
β(°)	90.511(2)	92.470(2)	92.10(4)
γ(°)	56.471(2)	55.531(2)	55.84(3)
V(Å^3)	753.13(6)	780.08(6)	787.183
Z	1	1	1
ρ_{cal}(g/cm^3)	6.38	6.49	6.42
λ (Å)	0.71073	0.71073	1.5418
μ (mm^{-1})	56.02	56.58	
2θ range for data collection	≤65.24	≤69.3	
No. of reflections collected	32373	14248	
No. of independent reflections	5286	6319	2790
No. of reflections with $I > 2\sigma(I)$	4543	5022	2428
No. of parameters refined	243	242	
R(int)	0.042	0.036	
Final R_1, wR_2 factors [$I > 2\sigma(I)$]	0.031, 0.073	0.034, 0.062	0.041
Final R_1, wR_2 factors (all data)	0.041, 0.076	0.050, 070	
Goodness-of-fit	1.093	1.013	
Reference	(1)	(2)	(3)

Reference: (1) This work; (2) Yang *et al.* (2007); (3) McLean & Anthony (1970).

TABLE 3. COORDINATES AND DISPLACEMENT PARAMETERS OF ATOMS IN RAYGRANTITE

Atom	*x*	*y*	*z*	U_{eq}	U_{11}	U_{22}	U_{33}	U_{23}	U_{13}	U_{12}
Pb1	0.25929(4)	0.11301(4)	0.25132(4)	0.01533(8)	0.0136(2)	0.0155(2)	0.0121(1)	0.0061(1)	–0.0053(1)	–0.0090(1)
Pb2	0.26564(4)	0.08114(4)	0.64895(3)	0.01200(7)	0.0104(1)	0.0102(1)	0.0117(1)	0.0050(1)	–0.0023(1)	–0.0062(1)
Pb3	0.92660(4)	0.23610(4)	0.02931(3)	0.01273(7)	0.0149(2)	0.0127(1)	0.0123(1)	0.0073(1)	–0.0040(1)	–0.0097(1)
Pb4	0.72237(4)	0.41691(4)	0.75348(4)	0.01446(8)	0.0154(2)	0.0172(2)	0.0161(2)	0.0118(1)	–0.0089(1)	–0.0113(1)
Pb5	0.31236(4)	0.46321(4)	0.53615(3)	0.01209(7)	0.0145(1)	0.0169(2)	0.0127(1)	0.0102(1)	–0.0078(1)	–0.0124(1)
Zn	0	0.5	0	0.0119(3)	0.0156(7)	0.0104(6)	0.0109(6)	0.0062(5)	–0.0045(5)	–0.0090(6)
S1	0.9580(3)	0.0793(3)	0.3619(2)	0.0107(4)	0.0131(9)	0.0122(9)	0.0096(8)	0.0056(8)	–0.0040(7)	–0.0102(8)
S2	0.5697(3)	0.1766(3)	0.1512(2)	0.0093(3)	0.0079(8)	0.0071(8)	0.0077(8)	0.0033(7)	–0.0007(7)	–0.0034(7)
S3	0.4433(3)	0.3275(3)	0.8370(2)	0.0096(3)	0.0093(8)	0.0109(9)	0.0108(8)	0.0066(8)	–0.0036(7)	–0.0073(7)
Si	0.0259(3)	0.4474(3)	0.6572(3)	0.0077(4)	0.0098(10)	0.0099(10)	0.0077(9)	0.0069(8)	–0.0041(8)	–0.0069(9)
O1	0.7667(9)	0.2146(9)	0.4768(7)	0.019(1)	0.020(3)	0.021(3)	0.014(3)	0.006(3)	0.000(3)	–0.016(3)
O2	0.0929(10)	0.0688(9)	0.4360(8)	0.025(1)	0.029(4)	0.024(4)	0.030(4)	0.015(3)	–0.021(3)	–0.022(3)
O3	0.0017(9)	0.0971(8)	0.7301(7)	0.015(1)	0.020(3)	0.012(3)	0.013(3)	0.005(2)	–0.003(2)	–0.012(3)
O4	0.9727(10)	0.1230(9)	0.2571(8)	0.022(1)	0.028(4)	0.027(4)	0.015(3)	0.014(3)	–0.006(3)	–0.019(3)
O5	0.5321(9)	0.1389(8)	0.2552(7)	0.014(1)	0.018(3)	0.016(3)	0.013(3)	0.011(3)	–0.003(2)	–0.010(3)
O6	0.4389(9)	0.1985(9)	0.0717(7)	0.022(1)	0.013(3)	0.027(4)	0.018(3)	0.013(3)	–0.010(3)	–0.011(3)
O7	0.7616(8)	0.0297(8)	0.0375(7)	0.016(1)	0.008(3)	0.013(3)	0.018(3)	0.009(3)	–0.001(2)	–0.002(2)
O8	0.5482(9)	0.3422(8)	0.2466(8)	0.017(1)	0.016(3)	0.009(3)	0.024(3)	0.009(3)	–0.008(3)	–0.008(3)
O9	0.5779(8)	0.3031(9)	0.9108(8)	0.019(1)	0.010(3)	0.023(3)	0.024(3)	0.015(3)	–0.010(3)	–0.011(3)
O10	0.4526(9)	0.3892(9)	0.7476(8)	0.020(1)	0.028(4)	0.031(4)	0.023(3)	0.022(3)	–0.013(3)	–0.024(3)
O11	0.2490(8)	0.4725(8)	0.9598(7)	0.014(1)	0.013(3)	0.010(3)	0.009(3)	0.001(2)	0.001(2)	–0.006(2)
O12	0.4688(9)	0.1611(8)	0.7378(8)	0.018(1)	0.012(3)	0.013(3)	0.019(3)	0.005(3)	–0.004(3)	–0.008(3)
O13	0.2242(8)	0.2933(8)	0.5076(6)	0.013(1)	0.011(3)	0.013(3)	0.006(2)	0.000(2)	0.003(2)	–0.008(2)
O14	0.0338(8)	0.3846(7)	0.7657(6)	0.011(1)	0.014(3)	0.009(3)	0.009(3)	0.007(2)	–0.005(2)	–0.006(2)
O15	0.9897(8)	0.3735(8)	0.2571(7)	0.012(1)	0.015(3)	0.007(3)	0.012(3)	0.005(2)	–0.002(2)	–0.007(2)
O16	0.8516(8)	0.4772(8)	0.6090(7)	0.014(1)	0.011(3)	0.019(3)	0.018(3)	0.015(3)	–0.010(2)	–0.010(3)
O17	0.1363(8)	0.2497(7)	0.9300(6)	0.009(1)	0.014(3)	0.007(3)	0.009(3)	0.006(2)	–0.005(2)	0.007(2)

TABLE 4. SELECTED BOND DISTANCES IN RAYGRANTITE

		Distance (Å)			Distance (Å)			Distance (Å)
S1	–O2	1.467(7)	Pb1	–O13	2.347(6)	Pb4	–O8	2.474(6)
	–O1	1.473(7)		–O15	2.558(6)		–O16	2.520(6)
	–O4	1.478(6)		–O4	2.610(7)		–O1	2.531(6)
	–O3	1.494(6)		–O5	2.711(6)		–O10	2.694(6)
	Ave.	1.478		–O12	2.761(6)		–O14	2.730(6)
				–O7	2.767(6)		–O11	2.777(6)
S2	–O6	1.467(6)		–O2	2.925(7)		–O3	2.909(6)
	–O7	1.470(6)		–O6	3.052(7)		–O6	3.008(7)
	–O8	1.484(6)		–O9	3.326(6)		–O9	3.137(7)
	–O5	1.490(6)		–O6	3.348(7)		–O9	3.236(7)
	Ave.	1.478		Ave.	2.840		–O2	3.275(7)
							Ave.	2.845
S3	–O9	1.453(6)	Pb2	–O14	2.325(6)			
	–O10	1.472(6)		–O17	2.454(5)	Pb5	–O16	2.268(5)
	–O12	1.475(6)		–O3	2.500(6)		–O13	2.350(6)
	–O11	1.515(6)		–O12	2.505(6)		–O15	2.563(6)
	Ave.	1.479		–O2	2.791(6)		–O5	2.713(6)
				–O5	2.850(6)		–O10	2.883(6)
Si	–O16	1.608(6)		–O1	3.074(6)		–O8	3.006(7)
	–O14	1.630(6)		–O13	3.284(6)		–O4	3.091(7)
	–O15	1.644(6)		–O12	3.509(7)		–O8	3.140(6)
	–O13	1.649(6)		Ave.	2.810		–O1	3.339(6)
	Ave.	1.633					–O1	3.362(7)
							Ave.	2.872
Zn	–O17	1.994(5) ×2	Pb3	–O17	2.352(6)			
	–O14	2.111(5) ×2		–O15	2.436(6)			
	–O11	2.181(6) ×2		–O7	2.476(6)			
	Ave.	2.096		–O11	2.656(6)			
				–O3	2.674(6)			
				–O10	3.074(7)			
				–O4	3.154(7)			
				–O4	3.228(6)			
				–O9	3.313(6)			
				–O7	3.443(6)			
				–O8	3.475(6)			
				Ave.	2.934			

The number and locations of the OH groups were determined from the bond-valence sum calculations. During the structure refinement, the ratio of the two twin domains was also refined to 0.64:0.36. Final coordinates and displacement parameters of the atoms in raygrantite are listed in Table 3 and selected bond-distances in Table 4.

Discussion

Crystal Structure

Raygrantite, $Pb_{10}Zn(SO_4)_6(SiO_4)_2(OH)_2$, is isotypic with iranite $Pb_{10}Cu(CrO_4)_6(SiO_4)_2(OH)_2$ (Yang *et al*. 2007) and hemihedrite $Pb_{10}Zn(CrO_4)_6(SiO_4)_2F_2$ (McLean & Anthony 1970) (Table 2). Its structure contains 10 symmetrically independent non-H cation sites, with five occupied by Pb^{2+} (Pb1, Pb2, Pb3, Pb4, and Pb5), three by S^{6+} (S1, S2, and S3), one by Si^{4+}, and one by Zn^{2+}. The SO_4 and SiO_4 tetrahedra and $ZnO_4(OH)_2$ octahedra form layers parallel to (120), which are linked together by Pb^{2+} cations displaying a wide range of Pb–O bond distances (Fig. 5, Table 4). The $ZnO_4(OH)_2$ octahedra are corner-linked to two symmetrically equivalent SO_4 and two SiO_4 tetrahedra, while two additional nonequivalent SO_4 groups (S1 and S2) are isolated (Fig. 6). As measured by the octahedral quadratic elongation (OQE) parameter (Robinson *et al*. 1971), the $CuO_4(OH)_2$ octahedron in iranite is more distorted (1.015) than the $ZnO_4(OH)_2$ octahedron in raygrantite (1.010) or the ZnO_4F_2

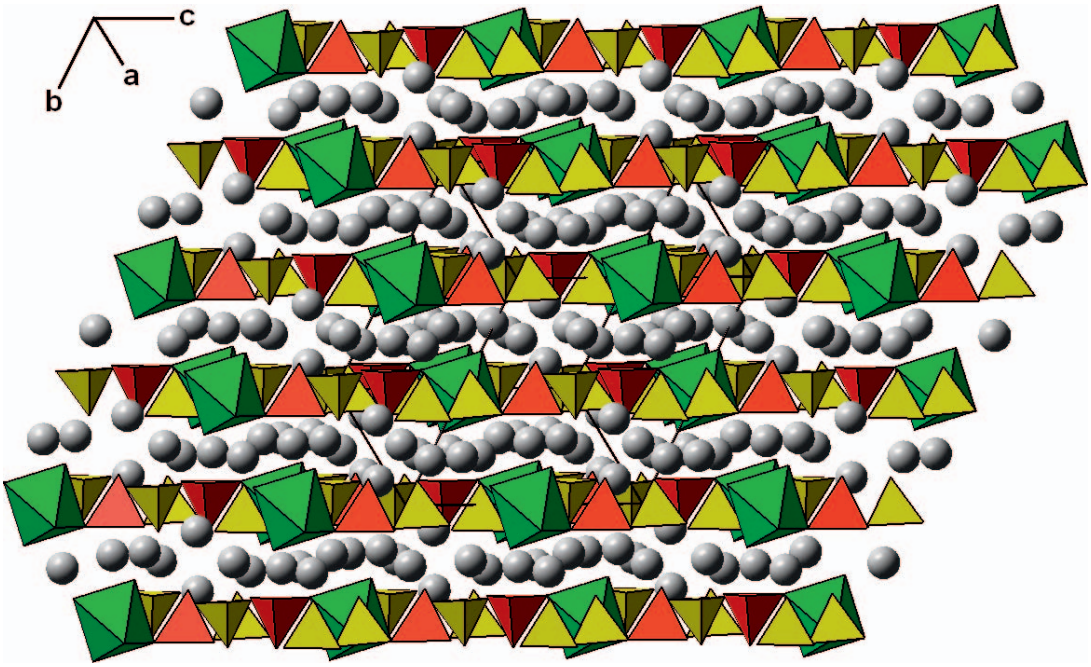

FIG. 5. Crystal structure of raygrantite. The yellow and red tetrahedra, green octahedra, and gray spheres represent SO_4, SiO_4, $ZnO_4(OH)_2$, and Pb, respectively.

octahedron (1.008) in hemihedrite, likely a consequence of the Jahn-Teller effect of Cu^{2+} (Yang *et al.* 2007).

From bond-valence considerations for iranite, Yang *et al.* (2007) showed that atom O17 represents the OH group with a hydrogen bond to O6 [O17–O6 = 2.852(6) Å]. The O17 site is also where the F atom is situated in hemihedrite (McLean & Anthony 1970). The same conclusion can be drawn for raygrantite, based on the calculations of the bond-valence sums

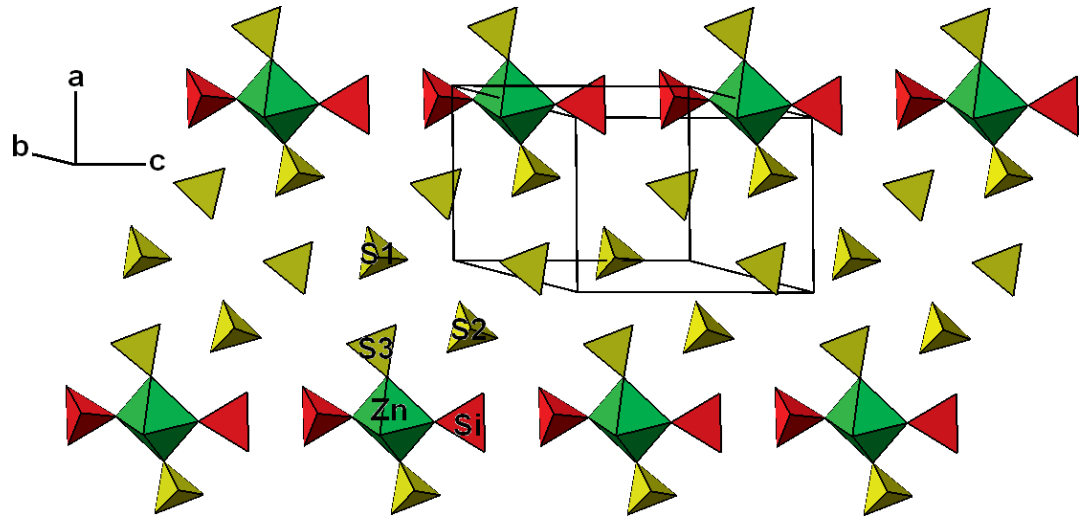

FIG. 6. A polyhedral layer in raygrantite. The yellow and red tetrahedra and green octahedra represent SO_4, SiO_4, and $ZnO_4(OH)_2$ groups, respectively.

TABLE 5. CALCULATED BOND-VALENCE SUMS FOR RAYGRANTITE

	Pb1	Pb2	Pb3	Pb4	Pb5	Zn	S1	S2	S3	Si	Sum
O1		0.07		0.32	0.04		1.50				1.96
					0.03						
O2	0.11	0.16		0.04			1.53				1.84
O3		0.35	0.22	0.12			1.43				2.11
O4	0.26		0.06		0.07		1.48				1.92
			0.05								
O5	0.20	0.14			0.20			1.44			1.98
O6	0.08			0.09				1.53			1.74
	0.04										
O7	0.17		0.37					1.52			2.09
			0.03								
O8			0.03	0.38	0.09			1.46			2.02
					0.06						
O9	0.04		0.04	0.06					1.59		1.78
				0.05							
O10			0.07	0.21	0.13				1.51		1.92
O11			0.23	0.17		0.28			1.34		2.02
						0.28↓					
O12	0.17	0.35							1.50		2.04
		0.02									
O13	0.53	0.04			0.53					0.93	2.03
O14		0.56		0.19		0.33				0.98	2.06
						0.33↓					
O15	0.30		0.42		0.30					0.95	1.97
O16				0.33	0.66					1.04	2.03
O17		0.40	0.52			0.46					1.38
						0.46↓					
Sum	1.90	2.09	2.04	1.95	2.09	2.14	5.94	5.94	5.94	3.91	

using the parameters given by Brese & O'Keeffe (1991) (Table 5). In raygrantite, O17 is the only O atom that does not participate in tetrahedral coordination with S^{6+} or Si^{4+}. The O17–O6 distance (3.108 Å) in raygrantite is longer than that in iranite [2.852(6) Å]. A comparison of the environment around O17 in iranite or raygrantite with that around the F atom in hemihedrite indicates that the bonding topologies of these ions are rather alike, suggesting no impediment to a complete solid solution between OH and F in hemihedrite, iranite, or raygrantite. Accordingly, we may postulate the possible existence of the OH-analogue of hemihedrite and the F-analogues of iranite and raygrantite, as well as the Cu-analogue of raygrantite. In fact, Cesbron & Williams (1980) successfully synthesized iranite, $Pb_{10}Cu(CrO_4)_6(SiO_4)_2(OH)_2$, and the OH-analogue of hemihedrite, $Pb_{10}Zn(CrO_4)_6(SiO_4)_2(OH)_2$, hydrothermally at 230 °C and in a pH range between 9 and 9.5, and concluded that a complete solid solution exists between iranite and the OH-analogue of hemihedrite.

Raman spectra

Displayed in Figure 7 is the Raman spectrum of raygrantite. Based on the Raman spectroscopic measurements on iranite and hemihedrite by Frost (2004), we made the following tentative assignments of major Raman bands for raygrantite: The relatively broad band at 3515 cm^{-1} can be ascribed to the O–H stretching vibrations. The bands between 800 and 1200 cm^{-1} are due to the S–O and Si–O stretching vibrations within the SO_4 and SiO_4 tetrahedral groups, whereas the bands between 380 and 660 cm^{-1} are primarily attributable to the O–S–O and O–Si–O bending vibrations. The bands below 350 cm^{-1} are of a complex nature and are mostly associated with the rotational and translational modes of SO_4 and SiO_4 tetrahedra, Zn–O interactions, and the lattice vibrational modes. According to Libowitzky (1999), an O–H···O distance of 3.1 Å would correspond to an O–H stretching frequency of ~3500 cm^{-1}, which is close to the value of 3515 cm^{-1} we measured for raygrantite.

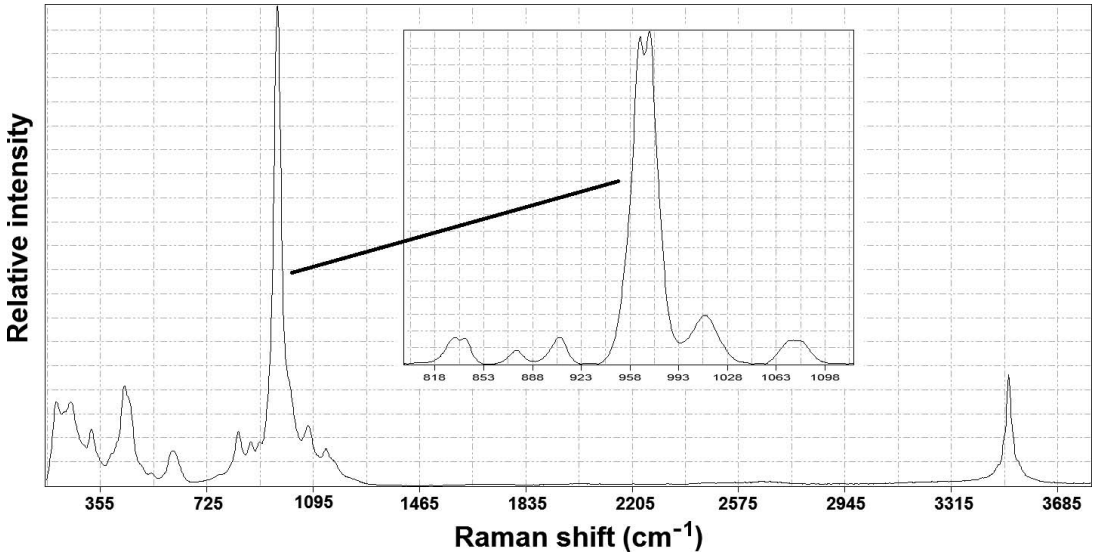

FIG. 7. Raman spectrum of raygrantite.

The complete substitution of S^{6+} for Cr^{6+} has been found in a number of mineral systems, such as the $BaCrO_4$ (hashemite) – $BaSO_4$ (barite) and $Pb_2O(CrO_4)$ (phoenicochroite) – $Pb_2O(SO_4)$ (lanarkite) solid solutions. Through hydrothermal synthesis, Cesbron & Williams (1980) found that it was possible to partially replace some of the $(CrO_4)^{2-}$ groups by $(SO_4)^{2-}$ groups and the resulting crystals, all of them twinned, contain about 6 wt.% SO_3, or 2.2 S *apfu*. The discovery of raygrantite indicates that, in addition to the complete OH–F and Cu–Zn substitutions, there is also a complete substitution between $(CrO_4)^{2-}$ and $(SO_4)^{2-}$ in the iranite group of minerals, pointing to the possible existence of a number of other $(SO_4)^{2-}$-bearing phases yet to be found or synthesized in this mineral group.

ACKNOWLEDGMENTS

This study was funded by the Science Foundation Arizona and the Sao Paulo Research Foundation (Grant: 2013/03487-8).

REFERENCES CITED

ALLEN, G.B. (1985) Economic Geology of the Big Horn Mountains of West-Central Arizona. Arizona Geological Survey, Open File Report **85–17**.

BRESE, N.E. & O'KEEFFE, M. (1991) Bond-valence parameters for solids. *Acta Crystallographica* **B47**, 192–197.

CESBRON, F. & WILLIAMS, S.A. (1980) Iranite-hémihédrite, bellite, phoenicochroite, vauquelinite et fornacite: synthèse et nouvelles données. *Bulletin de Minéralogie* **103**, 469–477.

DOWNS, R.T., BARTELMEHS, K.L., GIBBS, G.V., & BOISEN, M.B., JR. (1993) Interactive software for calculating and displaying X-ray or neutron powder diffractometer patterns of crystalline materials. *American Mineralogist* **78**, 1104–1107.

FROST, R.L. (2004) Raman microscopy of selected chromate minerals. *Journal of Raman Spectroscopy* **35**, 153–158.

LIBOWITZKY, E. (1999) Correlation of O–H stretching frequencies and O–H···O hydrogen bond lengths in minerals. *Monatshefte für Chemie* **130**, 1047–1059.

MCLEAN, W.J. & ANTHONY, J.W. (1970) The crystal structure of hemihedrite. *American Mineralogist* **55**, 1103–1114.

ROBINSON, K., GIBBS, G.V., & RIBBE, P.H. (1971) Quadratic elongation, a quantitative measure of distortion in coordination polyhedra. *Science* **172**, 567–570.

SHELDRICK, G.M. (2007) *TWINABS*. University of Göttingen, Göttingen, Germany.

SHELDRICK, G.M. (2008) A short history of *SHELX*. *Acta Crystallographica* **A64**, 112–122.

YANG, H., SANO, J.L., EICHLER, C., DOWNS, R.T., & COSTIN, G. (2007) Iranite, $CuPb_{10}(CrO_4)_6(SiO_4)_2(OH)_2$, isomorphous with hemihedrite. *Acta Crystallographica* **C63**, i122–i124.

Received May 5, 2015. Revised manuscript accepted October 14, 2015.